Infrared laser absorption spectroscopy of the $\nu_4(\sigma_u)$ fundamental and associated $\nu_{11}(\pi_u)$ hot band of C_7: Evidence for alternating rigidity in linear carbon clusters

J. R. Heath[a] and R. J. Saykally
Department of Chemistry, University of California, Berkeley, California 94720

(Received 23 August 1990; accepted 15 October 1990)

The first characterization of the bending potential of the C_7 cluster is reported via the observation of the $v = 1^1$ and $v = 2^0$ levels of the $\nu_{11}(\pi_u)$ bend as hot bands associated with the $\nu_4(\sigma_u)$ antisymmetric stretch fundamental. The lower state hot band rotational constants are measured to be 1004.4(1.3) and 1123.6(9.0) MHz, constituting a 9.3% and 22% increase over the ground state rotational constant [918.89(41) MHz]. These large increases are strong evidence for extremely large amplitude, anharmonic bending modes in this cluster. In addition, quartic and sextic centrifugal distortion constants determined for the ground and $\nu_4 = 1$ states are found to be anomalously large and negative, evidencing strong perturbations between stretching and bending modes.

INTRODUCTION

Small carbon clusters ($n < = 11$) are calculated to have low-lying linear electronic states with very low frequency bending modes,[1-5] which profoundly influence their kinetic and thermodynamic properties. On the basis of simple MO symmetry arguments, the degree of nonrigidity of these clusters about the central carbon atom is predicted to alternate regularly with cluster size.[4,6] In particular, clusters having a filled HOMO of π_u symmetry (e.g., C_3, C_7, C_{11}) are predicted to exhibit attractive overlap of the valence orbitals upon bending about the center of symmetry. Conversely, those with a filled π_g HOMO (e.g., C_5, C_9) have a higher energy barrier to bending about the central carbon atom, since this distortion forces a repulsive overlap of the + and − lobes of the (valence) wave function. Brown and Lipscomb[6] have calculated bending force constants for the C_n ($n = 3,5,7$) and C_nO_2 ($n = 1,3,5$) series, and their results strongly support this picture.[6] This simple qualitative model is both interesting and useful; however, while it correctly predicts the experimentally observed rigidity of CO_2 (Ref. 7) and nonrigidity of C_3O_2,[7,8] the predictions for linear carbon clusters are only just beginning to be tested over a meaningful range of cluster sizes.

Over the past two years a number of research groups have performed high resolution spectroscopic measurements of the $^1\Sigma_g$ ground electronic state vibrational manifold of C_3.[9-12] This cluster has been found to be highly nonrigid, possibly even quasilinear. The first precise spectroscopic measurements of the $^1\Sigma_g$ ground electronic state of C_5 were published last year by three groups.[13-15] Moazzen-Ahmadi and co-workers have measured bending hot bands associated with the ν_3 (σ_u) antisymmetric stretch of C_5.[16] Their measurements indicate that C_5 is quite rigid, and has relatively harmonic bending potentials. We recently reported the first measurement of the structure and infrared frequencies of the $^1\Sigma_g$ ground state of C_7 using diode laser absorption spectroscopy of a supersonic carbon cluster jet.[17] In that article we reported 36 lines of the highest frequency $\nu_4(\sigma_u)$ antisymmetric stretch. We have now improved our sensitivity sufficiently to enable measurement of the $(0001000^00^00^00^01^1) \leftarrow (0000000^00^00^00^01^1)$ and the $(0001000^00^00^00^02^0) \leftarrow (0000000^00^00^00^02^0)$ bending hot bands associated with the ν_4 fundamental. This constitutes the first characterization of the bending potential of C_7. Excitation to $v = 1^1$ of the $\nu_{11}(\pi_u)$ bending fundamental is accompanied by a huge increase (9.3%) in the rotational constant. Excitation from $v = 1^1$ to $v = 2^0$ of ν_{11} results in an even larger increase (10.4%) in the rotational constant. The magnitude of these changes indicates extremely large amplitude bending motion about the central carbon atom, evidencing the predicted nonrigidity of C_7. In addition, the ν_4 rotational transitions have been measured with improved precision and extended to $J = 64$ in the P branch and $J = 54$ in the R branch. This allows for a more accurate band analysis and for determination of upper and lower state quartic and sextic centrifugal distortion constants for the fundamental transition. These distortion constants are found to be negative, indicative of perturbations by excited bending states.

EXPERIMENTAL

A schematic of the experimental apparatus is shown in Fig. 1. The cluster source has been optimized to produce an intense gas-dynamically focused supersonic jet of cold carbon clusters. The cluster jet is generated by cylindrically focusing 200–300 mJ of a KrF excimer laser (248 nm) to a 0.5 mm × 7 mm line on a graphite target placed in the throat of a pulsed planar nozzle (1.5 mm × 10 mm). The carrier gas pulse is generated by a General Valve (1.5 mm diam orifice) Series 9 Pulsed Valve, which is backed with 20 atm of argon, and fired such that maximum carrier gas density passes over the graphite target in coincidence with the laser ablation. The Ar carrier entrains and cools the carbon clusters, and the cluster/gas beam expands into a vacuum chamber

[a] UC Berkeley Miller Research Fellow, 1988–1990.

 0021-9606/91/031724-06$03.00

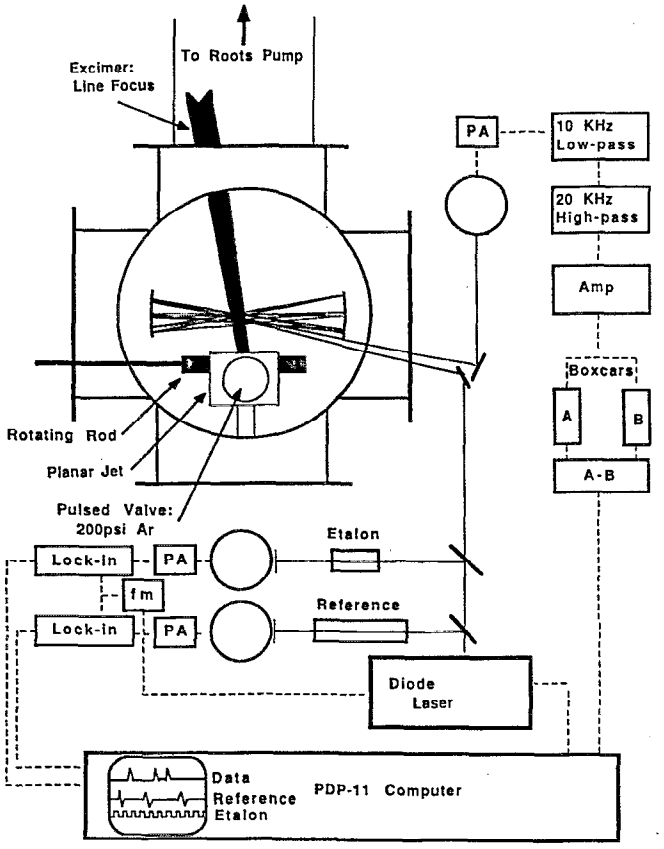

FIG. 1. Schematic of apparatus designed for infrared diode laser absorption spectroscopy of a supersonic carbon cluster jet. In this experiment, C_7 clusters were generated by excimer laser (248 nm) ablation of a graphite target placed in the throat of a gas-dynamically focused supersonic slit nozzle. The clusters intersect 10–12 passes of a diode laser approximately 1–2 cm downstream from the nozzle orifice. The infrared transitions are detected as a 15 μs wide absorption transient by gated detection with two boxcar signal averagers. Absolute and relative signal calibrations are performed simultaneously with the measurement of the C_7 absorption spectrum. The experiment is cycled at 80–100 Hz.

pumped by a 2800 cfm Roots pump, where it intersects 10–12 passes of an infrared diode laser beam. The diode laser multipass optical cell is designed after that of Karu and coworkers.[18] The diode laser beam bisects the cluster beam in a narrow spatial region ($\sim$5 mm) and with very little angular dispersion ($< 10°$) between the diode laser and the molecular beam. This optical cell design maximizes the absorption signal amplitude and minimizes the Doppler width of the absorption line shape. Absorption resonances are detected by monitoring the diode laser power with an InSb detector. The diode laser is typically incremented by 15–20 MHz after signal averaging for 30–60 excimer shots.

In large part, the experimental difficulty involved in the spectroscopy of these clusters lies in the transient nature of the absorption signals. The pulsed carbon cluster beam passes through the multipass optical cell in about 15 μs. When this is coupled to an experimental repetition rate of 100 Hz, the effective duty cycle of the experiment is only 0.15%, and the corresponding frequency spectrum of an absorption signal is extremely broad. It is difficult to filter diode laser and detector noise without significantly altering the time profile and amplitude of an absorption signal. This problem has been addressed by careful selection of high- and low-pass signal filters (10 and 20 kHz, respectively). Such filtering reduces the detector and laser noise by approximately a factor of 100 while maintaining the 15 μs absorption signal profile and 70% of the absorption signal amplitude. The filters do, however, ac couple the signal, giving it both positive and negative voltage components. Two boxcar signal averagers are triggered 12 μs apart, and each samples the amplified and filtered detector output for 3 μs. When the laser is on resonance the boxcars sum negative and positive signal components, and when the laser is off resonance the boxcars subtract background fluctuations.

Absorption linewidths of 45 MHz (FWHM) may be observed by rapidly scanning a diode laser (ten excimer shots per diode laser step) setup in a single pass configuration. For the experiments reported here, however, the linewidth is 60–100 MHz. This linewidth increase comes from three sources: (1) increased Doppler width from the use of the multipass cell; (2) increased frequency jitter of the diode laser during a longer scan; and (3) a 100–300 shot time constant applied to the boxcar averagers for purposes of noise reduction.

The ultimate detection sensitivity of this apparatus was measured to be about 2–3 parts in 10^5 for a 300 shot scan with a 1000 shot boxcar time constant. The cluster source produces carbon clusters at rotational temperatures which vary between 10–25 K.

Absolute and relative frequency calibrations are performed by splitting off part of the diode laser beam and simultaneously recording both the absorption spectrum of N_2O (Ref. 19) in a static gas cell and the fringe spectrum of a temperature stabilized air-spaced germanium etalon. In order to do this, a small amplitude ($\sim$15 MHz) 100 kHz frequency modulation is applied to the diode laser. The N_2O reference gas and the germanium etalon spectra are detected by lock-in amplification. This slight frequency modulation does not affect the signal to noise of the transient absorption signal. Uncertainties in frequency measurements, dominated by frequency drift of the diode laser, range from 0.001 to 0.003 cm^{-1}. This is dependent upon the individual diode, the particular mode of that diode, and the rate at which frequency is scanned.

RESULTS

A typical scan showing absorption features of both the ν_4 fundamental and the associated ν_{11} hot band ($v = 1$) is shown in Fig. 2. Observed frequencies assigned to the ν_4 fundamental are listed in Table I. The ν_4 fundamental was fit to the expression

$$E = (v + 1/2)\nu + B_v[J(J+1)] - D_v[J(J+1)]^2 + H_v[J(J+1)]^3 \quad (1)$$

in a least squares analysis. Fitted molecular constants for these transitions are listed in Table II. The negative centrifugal distortion constants presented in Table II are unusual for low-lying states of a strongly bound molecule, hence variations of this analysis were performed in order to check for

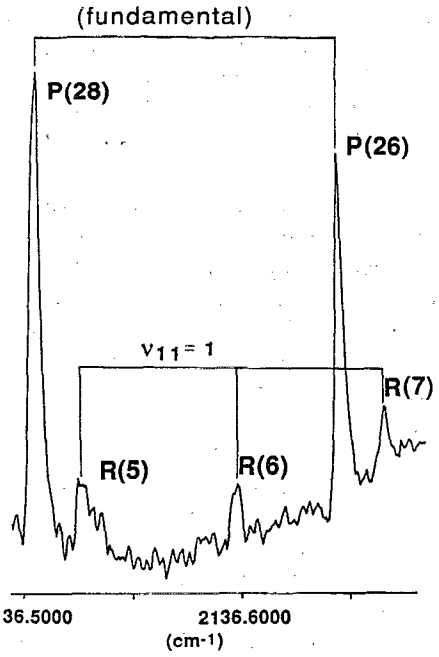

FIG. 2. Typical data showing two rovibrational lines of the ν_4 (σ_u) antisymmetric stretch fundamental of C_7 and three lines of an associated hot band assigned to $v = 1^1$ of the ν_{11} (π_u) degenerate bending fundamental. Note that the frequency scale is not exactly linear.

TABLE I. Observed frequencies assigned to the ν_4 (σ_u) antisymmetric stretch fundamental of C_7. The standard deviation of the fit was 0.0018 cm^{-1}.

J	$R(J)$	obs-calc ($\times 10^{-3}$)	$P(J)$	obs-calc ($\times 10^{-3}$)
0	2138.3771	0.8		
2	2138.4954	− 2.1	2138.1928	0.2
4	2138.6188	0.9	2138.0695	0.6
6	2138.7409	3.6	2137.9472	2.9
8	2138.8565	0.6	2137.8205	1.7
10	2138.9704	− 3.0	2137.6929	0.6
12	2139.0881	1.9	2137.5611	− 3.8
14	2139.2079	− 3.4	2137.4348	− 1.7
16	2139.3174	0.9	2137.3077	0.5
18	2139.4358	− 1.1	2137.1793	2.3
20	2139.5469	− 0.0	2137.0444	− 1.3
22	2139.6602	0.1	2136.9130	− 0.6
24	2139.7718	0.1	2136.7800	− 0.5
26			2136.6465	− 0.0
28	2139.9922	0.5	2136.5116	− 0.0
30	2140.0989	− 1.5	2136.3720	− 3.8
32	2140.2110	2.8	2136.2410	1.9
34	2140.3137	− 1.3	2136.1034	− 1.9
36	2140.4216	0.7	2135.9619	− 1.1
38	2140.5278	2.0	2135.8246	0.9
40	2140.6313	1.7	2135.6851	1.7
42	2140.7320	− 0.3	2135.5435	1.3
44	2140.8325	− 1.6	2135.3978	− 2.4
46	2140.9342	− 0.4	2135.2595	2.1
48	2141.0327	− 1.2	2135.1124	− 1.2
50	2141.1306	− 1.2	2134.9685	− 0.5
52	2141.2286	0.2	2134.8229	− 0.6
54	2141.3248	1.3	2134.6776	0.5
56			2134.5288	− 1.0
58			2134.3804	− 1.2
60			2134.2337	1.3
62			2134.0844	2.2
64			2133.9293	− 1.6

TABLE II. Molecular constants for the ν_4 (σ_u) antisymmetric stretch fundamental of C_7. Quoted uncertainties are 1σ.

ν_4	2138.3152(5) cm^{-1}
B''	917.80(44) MHz
D''	− 0.71(27) kHz
H''	− 0.167(44) Hz
B'	914.29(48) MHz
D'	− 0.77(29) kHz
H'	− 0.184(51) Hz

artifacts. When the data were fit with exclusion of the distortion parameters the standard deviation of the fit was only about 20% worse. Systematic errors were, however, observed in the fit at high J. The correlation matrix for the fit of Table II indicates that the upper and lower state constants are highly correlated, consequently the upper state and lower state constants were fit separately from combination differences in order to minimize these effects. Distortion constants thus calculated were, in fact, slightly better determined, but they were still well within the statistical limits (1σ) of those presented in Table II. Hence, the results of the initial fit are retained here.

Transition frequencies assigned to the ν_{11} hot bands are listed in Tables III and IV, and the corresponding molecular constants are listed in Table V. As only a limited number of these transitions were observed, centrifugal distortion constants were not determined, and the data were fit to the standard expression

$$E = (v + 1/2)\nu + B_v[J(J+1) - l^2]. \quad (2)$$

It was not possible to resolve the l-doubling constant (q), and therefore, the ν_{11} (π_u) bending frequency could not be estimated from the relationship $\nu = 2.1(B_0^2/q)$.[16] The lowest frequency hot band (Table III) was assigned to the ν_{11} bending fundamental for two reasons: (1) both even and odd J values are observed, so the transition must originate from a degenerate bend; (2) the enormous increase (9.3%) in the lower state rotational constant of this transition relative to the ground state rotational constant of C_7,

TABLE III. Measured frequencies for $v = 1$ ($l = 1$) of the ν_{11} (π_u) hot band associated with the ν_4 highest frequency (σ_u) antisymmetric stretch of C_7.

J	$R(J)$	obs-calc ($\times 10^{-3}$)	$P(J)$	obs-calc ($\times 10^{-3}$)
2	2136.3315	− 3.7		
3	2136.4031	1.6	2135.9349	0.9
4	2136.4654	− 2.1	2135.8678	1.4
5	2136.5343	0.9	2135.7973	− 1.4
6	2136.5988	− 0.3	2135.7331	2.3
7	2136.6686	4.0	2135.5948	0.4
8	2136.7316	1.7	2135.5225	− 3.5
9	2136.7949	− 0.1	2135.4600	2.6
10	2136.8581	− 1.8	2135.3878	− 0.7
11	2136.9240	− 0.7		

TABLE IV. Measured frequencies for $v=2$ ($l=0$) of the ν_{11} (π_u) hot band associated with the ν_4 (σ_u) highest frequency antisymmetric stretch of C_7. No lines of the p branch were observed (due to insufficient frequency coverage).

J	$R(J)$	obs-calc ($\times 10^{-3}$)
2	2134.0279	2.5
4	2134.1705	−2.4
6	2134.3178	−1.7
8	2134.4653	0.1
12	2134.7539	0.7
14	2134.8976	1.9
16	2135.0378	0.6
18	2135.1755	−2.1
20	2135.3173	0.3

can reasonably result only from motion in the ν_{11} coordinate (bending about the central carbon). Raghavachari and Binkley[2] have calculated the ν_{11} bend of C_7 to lie at 73 cm^{-1}.[2] C_7 does have a number of other low-frequency bends, predicted at 157 (π_g), 240 (π_u), 598 (π_g), and 710 (π_u) cm^{-1}. These vibrations are likely to be less populated in a cold supersonic jet, and no evidence of hot bands arising from these modes was observed. A simple calculation which assumes a 30–50 K vibrational temperature (observed for C_3) and a Boltzmann distribution of occupied vibrational levels indicates that the observed hot bands come from a vibration which lies at around 50–110 cm^{-1}, consistent with the *ab initio* prediction for ν_{11}. The other hot band observed (Table IV) was tentatively assigned to ν_{11} ($v=2^0$) based on the following evidence: (1) the band origin shift is approximately twice that of the $v=1^1$ hot band; (2) only even J values are observed; and, (3) the increase in the lower state rotational constant relative to the ground state value (22%) is about twice that observed for the $v=1^1$ band. This assignment is somewhat suspect, as only the R branch of this transition was observed due to inadequate diode laser frequency coverage, and the band origin determination is only approximate (± 0.3 cm^{-1}). Shifting the rotational assignment by a few J does not significantly affect either the standard deviation of the least squares fit or the calculated rotational constants. No transitions arising from the $v=2^2$ hot band were observed. This is probably due to inadequate sensitivity, as the transitions assigned to $v=2^0$ hot band were actually quite weak. It is, however, interesting to note that Moazzen-Ahmadi and co-workers[16] were similarly unable to detect the analogous $v=2^2$ hot band for C_5, even though the $v=2^0$ component was observed with a reasonable signal to noise ratio.

TABLE V. Molecular constants derived from least squares analysis of observed transitions assigned to $v=1$ ($l=1$) and $v=2$ ($l=0$) of the ν_{11} (π_u) hot band associated with the ν_4 (σ_u) highest frequency antisymmetric stretch of C_7.

Quantity	$v=1$ ($l=1$)	Hot band $v=2$ ($l=0$)
ν (cm^{-1})	2136.0687(9)	2133.8020(29)
B'' (MHz)	1006.8(1.2)	1123.6(9.0)
B' (MHz)	1004.0(1.0)	1119.9(8.3)

Rare gas matrix shifts for linear C_n

The difficulties involved with scanning diode lasers over large frequency ranges are well known. Therefore the gas phase experiments presented here and elsewhere for C_7,[17] C_3,[9] C_5,[13–16] and C_9[20] have been greatly aided by the work of Weltner and co-workers[1,21] who have reported on the infrared spectra of carbon clusters isolated in rare gas matrices. However, a molecule isolated in a rare gas matrix will usually exhibit a substantial, and usually unquantifiable, matrix-induced shift of an absorption band origin. If that matrix shift were systematic, then it could be corrected for, and the gas phase band origins could then be inferred from properly assigned matrix data. Such a systematic (red) shift is, in fact, observed for antisymmetric stretches of the linear C_n cluster series in argon matrices, and this is presented in Fig. 3 for the clusters ($n=3,5,7,9$). Matrix lines observed at 2040 and 2164 cm^{-1} have been assigned previously to C_3 (Ref. 21) and C_5.[22] With a little experimental hindsight, two other matrix lines at 2128 and 1997 cm^{-1} (previously assigned to C_9 and C_7) can be assigned to the ν_4 and ν_6 antisymmetric stretching fundamentals of C_7 and C_9, respectively. These assignments have also been proposed in recent theoretical work of Martin and co-workers.[23] The true (unperturbed) band origins for these transitions are 2040.0, 2169.4, 2138.3, and 2014.3 cm^{-1} for C_3, C_5, C_7, and C_9. A matrix line observed at 1893 cm^{-1} appears highly correlated with the 2128 cm^{-1} line associated with C_7. This 1893 cm^{-1} band is in good agreement with theoretical predictions for the ν_5 (σ_u) antisymmetric stretch fundamental of C_7, also predicted to be strongly allowed.[23,24] The correlation presented in Fig. 3 indicates that the unperturbed ν_5 band origin lies near 1902–1904 cm^{-1} assuming that similar matrix shifts will occur for both the ν_4 and ν_5 antisymmetric stretch modes.

DISCUSSION

The quartic and sextic distortion constants presented in Table II for the ground state and the $\nu_4=1$ state of C_7 are anomalous both in sign and magnitude. They may be compared directly to those of C_5 and C_3 by scaling with the appropriate rotational constants (D/B). The magnitudes of the scaled constants for C_7 are ~ 12 times larger than those for C_5, and only four times smaller than those for the highly nonrigid C_3 cluster, indicative of perturbations within both states of C_7. The vibrational manifold of C_3 is severely perturbed by stretch–bend and Coriolis interactions, which are manifested in the rotational constants, l-type doubling constants, and distortion parameters.[9–11,25,26] The slight band origin shift of the ν_{11} hot band from the ν_4 fundamental band origin, coupled with the small decrease in the rotational constant observed for the fundamental transition, in-

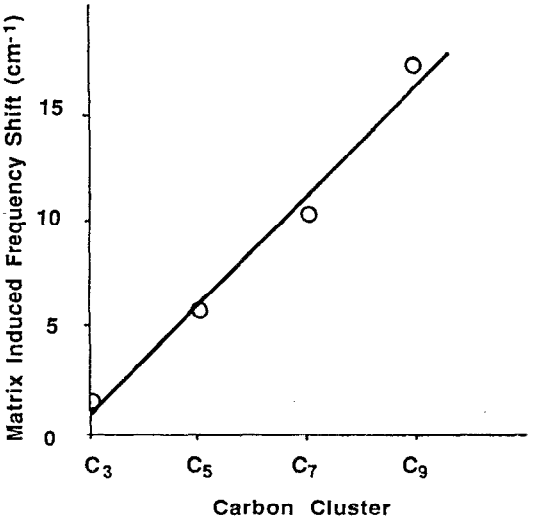

FIG. 3. Correlation showing matrix-induced shifts of antisymmetric stretch vibrational band origins for linear carbon clusters isolated in argon matrices vs carbon cluster size. The matrix shift is approximately 2.5 (n-3) cm^{-1} to the red of the true band origin for an n-atom cluster.

dicates that stretch–bend interactions (at least in the ν_4 coordinate) are significantly smaller in C_7 than in C_3. C_7 does have a predicted low-lying π_g bending fundamental, and hence the large, negative distortion parameters observed here for C_7 could arise from Coriolis interactions between the Σ_g ground state and excited levels of that mode. Measurements of the pure bending levels of C_7 by far-infrared laser spectroscopy, such as those reported recently for C_3,[12] will certainly help clarify this situation.

The large increase in the rotational constant of C_7 which accompanies excitation to the first two levels of the ν_{11} bend is, to our knowledge, unprecedented in strongly bound molecular systems. These changes in the C_7 rotational constants, and the corresponding properties for C_3, C_5, and the prototypical quasilinear molecule C_3O_2 are compared in Table VI.

The results presented in Table VI for C_5 are typical for a semirigid linear molecule. Those given for C_3 and C_7, however, evidence extremely large amplitude bending motion about the central carbon atom in these two clusters. The projection of the average length of a bent molecule on the primary axis of rotation will decrease linearly as the bending angle is decreased from 180°, whereas the effective rotational constant B_v changes as $1/r^2$. Thus, although the fractional changes in the rotational constant for C_7 are 3 to 5 times larger than those observed for C_3, the actual bending amplitude of C_7 is somewhat less than twice that of C_3. This large amplitude bending motion observed for both C_3 and C_7 is consistent with the molecular orbital symmetry argument discussed earlier.

Large amplitude bending motion may provide a mechanism through which odd-numbered cumulenes can isomerize to form monocyclic rings, which are the predicted ground state structures for $n > 9$.[6] It is interesting to note that the symmetry of the π_u HOMO in C_3, C_7, and C_{11} is appropriate for cumulene–monocyclic ring intramolecular isomerization. Thus, the activation barrier for isomerization of these singlet ground-state cumulenes would be expected to be lower than for the other linear carbon clusters. Such intraconversion may become quite facile by $n = 11$, where anion photoelectron spectroscopy indicates ring and linear isomers coexist.[27]

TABLE VI. Observed increases in the rotational constants (compared to the ground state B'') for $v = 1^1$ and $v = 2^0$ of the lowest frequency (π_u) bending modes for odd-numbered carbon clusters and the quasilinear molecule C_3O_2.

	$[(\Delta B)/B''] \times 100\%$	
	$\nu_b = 1^1$	$\nu_b = 2^0$
C_3	*f* 3.36%	4.9%
	e 2.1%	
C_5	0.36%	0.70%
C_7	9.3%	22%
C_3O_2	*e* 1.3%	0.92%
	f 0.72%	

ACKNOWLEDGMENTS

We are indebted to R. Cohen for many stimulating discussions and to Dr. D. Ewing and Dr. J. Martin for sending us their respective results prior to publication. We would also like to acknowledge the assistance of J. Kim and R. Sheeks. This work was funded in part by the Office of Naval Research (Grant No. N004-90-J-1368) and the NASA Innovative Science Program. J.R.H. thanks the Miller Foundation for support.

[1] W. Weltner, Jr. and R. J. Van Zee, Chem. Rev. **89**, 1713 (1989).
[2] K. Raghavachari and J. S. Binkley, J. Chem. Phys. **87**, 2191 (1987).
[3] D. W. Ewing and G. V. Pfeiffer, Chem. Phys. Lett. **86**, 365 (1981).
[4] Q. Fan and G. V. Pfeiffer, Chem. Phys. Lett. **162**, 472 (1989).
[5] J. M. L. Martin, J. P. Francois, and R. Gifbels, J. Chem. Phys. (in press).
[6] L. D. Brown and W. N. Lipscomb, J. Am. Chem. Soc. **99**, 3968 (1977).
[7] L. Fusina, I. M. Mills, and G. Guelachvilli, J. Mol. Spectrosc. **79**, 101 (1980).
[8] B. P. Winnewisser, in *Molecular Spectroscopy: Modern Research*, edited by K. N. Rao (Academic, Orlando, 1985), Vol. III, pp. 322–411.
[9] K. Kawaguchi, K. Matsumura, H. Kanamori, and E. Hirota, J. Chem. Phys. **91**, 1953 (1989).
[10] (a) R. S. Smith, M. Anselment, L. F. DiMauro, J. M. Frye, and T. J. Sears, J. Chem. Phys. **89**, 2591 (1988); (b) F. J. Northrup and T. J. Sears, Chem. Phys. Lett. **159**, 421 (1989); (c) J. Opt. Soc. Am. B 7 (in press).
[11] (a) E. A. Rohlfing, J. Chem. Phys. **89**, 6103 (1988); (b) E. A. Rohlfing and J. E. Goldsmith, *ibid.* **90**, 6804 (1989); (c) J. Opt. Soc. Am. B **7**, (in press).
[12] C. A. Schmuttenmaer, R. C. Cohen, N. Pugliano, J. R. Heath, A. L. Cooksy, K. L. Busarow, and R. J. Saykally, Science **249**, 897 (1990).
[13] J. R. Heath, A. L. Cooksy, M. H. W. Gruebele, C. A. Schmuttenmaer, and R. J. Saykally, Science **244**, 565 (1989).
[14] P. F. Bernath, K. H. Hinkle, and J. J. Keady, Science **244**, 562 (1989).
[15] N. Moazzen-Ahmadi, A. R. W. McKellar, and T. Amano, Chem. Phys. Lett. **157**, 1 (1989).
[16] N. Moazzen-Ahmadi, A. R. W. McKellar, and T. Amano, J. Chem. Phys. **91**, 2140 (1989).
[17] J. R. Heath, R. A. Sheeks, A. L. Cooksy, and R. J. Saykally, Science **249**, 895 (1990).

[18] D. Karu, A. M. De Souza, J. Wanna, and D. S. Perry, Appl. Opt. **29**, 119 (1990).
[19] G. Guelachvili and N. K. Rao, *Handbook of Infrared Standards* (Academic, Orlando, 1986).
[20] J. R. Heath and R. J. Saykally, J. Chem. Phys. **93**, 8392 (1990).
[21] K. R. Thompson, R. L. DeKock, and W. Weltner, Jr., J. Am. Chem. Soc. **93**, 4688 (1971).
[22] M. Vala, T. M. Chandrasekhar, J. Szcepanski, R. Van Zee, and W. Weltner, Jr., J. Chem. Phys. **90**, 595 (1989).
[23] J. M. L. Martin, J. P. Francois, and R. Gijbels, J. Chem. Phys. (submitted).
[24] D. W. Ewing (private communication).
[25] R. Beardsworth, P. R. Bunker, P. Jensen, and W. P. Kraemer, J. Mol. Spectrosc. **118**, 50 (1986).
[26] P. Jensen and W. P. Kraemer, J. Mol. Spectrosc. **129**, 172 (1988).
[27] S. H. Yang, C. L. Pettiette, J. Conceicao, O. Chesnovsky, and R. E. Smalley, Chem. Phys. Lett. **139**, 233 (1987).